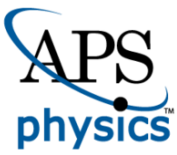

Ion-ion dynamic structure factor of warm dense mixtures

N. M. Gill, R. A. Heinonen, C. E. Starrett, and D. Saumon

Phys. Rev. E **91**, 063109 — Published 25 June 2015

DOI: 10.1103/PhysRevE.91.063109

Ion-ion dynamic structure factor of warm dense mixtures

N. M. Gill,[1,2] R. A. Heinonen,[2] C. E. Starrett,[2,*] and D. Saumon[2]

[1] *206 Allison Laboratory, Auburn University, Auburn, AL 36849*
[2] *Los Alamos National Laboratory, P.O. Box 1663, Los Alamos, NM 87545, U.S.A.*

The ion-ion dynamic structure factor of warm dense matter is determined using the recently developed pseudo-atom molecular dynamics method [Starrett *et al.* Phys. Rev. E 91, 013104 (2015)]. The method uses density functional theory to determine ion-ion pair interaction potentials that have no free parameters. These potentials are used in classical molecular dynamics simulations. This constitutes a computationally efficient and realistic model of dense plasmas. Comparison with recently published simulations of the ion-ion dynamic structure factor and sound speed of warm dense aluminum finds good to reasonable agreement. Using this method, we make predictions of the ion-ion dynamical structure factor and sound speed of a warm dense mixture – equimolar carbon-hydrogen. This material is commonly used as an ablator in inertial confinement fusion capsules, and our results are amenable to direct experimental measurement.

PACS numbers: 52.25.-b, 52.35.Dm, 52.65.Yy

I. INTRODUCTION

Typically, warm dense matter refers to plasmas that have temperatures of 1-100 eV and are 1-100 times solid density. It is a state of matter that exists in the interiors of giant planets [1], in the envelopes of white dwarfs [2], and in inertial confinement fusion experiments [3]. Due to the strong electron-electron, electron-ion and ion-ion interactions, it is very challenging to model. The last few years have seen an increased interest in modeling warm dense plasma mixtures, which occur in many systems of interest in nature and the laboratory. Ab initio simulation methods have been applied to the calculation of the equation of state and transport properties of D-T mixtures [4], LiH [5], and a variety of C-H mixtures [6–8].

The ion-ion dynamic structure factor embodies the space and time correlations of the ionic positions in the plasma. From it, one can in principle extract macroscopic information on state of the plasma, including the adiabatic sound speed and thermal diffusivity, which are essential input quantities for hydrodynamic simulations of plasmas. Predicting the ion-ion dynamic structure factor in warm dense matter has been the subject of a number of recent publications [9–12]. Its measurement using free-electron lasers [13, 14] is an imminent possibility, and will represent an unparalleled test of current models.

To date, predictions of the ion-ion dynamical structure factor $S_{\alpha\beta}(k,\omega)$ from simulations of warm dense matter have been made using either density functional theory (DFT) molecular dynamics (MD) [9, 10], or with classical molecular dynamics using model ion-ion pair interaction potentials with adjustable parameters [9, 11]. The former method, DFT-MD, is the state-of-the-art approach for modeling warm dense matter but suffers from being extremely expensive; typically a calculation at a single density-temperature point requires the use of massively parallel supercomputers. This limiting factor is particularly acute for the calculation of $S_{\alpha\beta}(k,\omega)$ since its evaluation suffers from numerical noise that can only be reduced by using long simulations and thousands of particles [12]. So far, DFT-MD simulations for $S_{\alpha\beta}(k,\omega)$ in the warm dense matter regime have been limited to hundreds of particles, relatively short simulation times, and to pure aluminum plasmas. In contrast, the relatively inexpensive pair potential based classical molecular dynamics simulations [9, 11] can use thousands of particles and long simulation times. However, their predictive capability is limited by their parametric potentials that are tuned so that the results match DFT-MD calculations [9]. Moreover, such matching has been shown to be problematic [15].

Recently, it has been shown that reliable, and parameter free, ion-ion pair interaction potentials can be calculated with DFT-based approach called pseudo-atom molecular dynamics (PAMD) [16]. These pair potentials are not tuned to DFT-MD simulations, but are the result of DFT-based average atom calculations. The average atom calculations proceed rapidly, and for a given plasma density, temperature and composition, pair potentials can be quickly generated without high-performance computing resources. These pair potentials have already been shown to give equation of state, diffusion coefficients and pair distribution functions in excellent agreement with DFT-MD simulations [16–18]. In this paper we use PAMD to make the first predictions of $S_{\alpha\beta}(k,\omega)$ in warm dense matter based on a parameter-free pair potentials. We compare to Kohn-Sham based DFT-MD simulations for aluminum [10], finding good agreement, and to Thomas-Fermi based DFT-MD simulations finding reasonable agreement. This is a further, very stringent test of the quality of the pair potentials obtained with this method. The result shows that accurate predictions of $S_{\alpha\beta}(k,\omega)$ in warm dense matter using parameter-free pair potentials in MD simulations are possible. Due to the vastly reduced computational expense, this opens the door to wide-ranging explorations of the ionic struc-

*Electronic address: starrett@lanl.gov

ture of dense plasmas, including mixtures, that can both guide and be tested by experiments [14].

Here we use PAMD to show that in the hydrodynamic limit of $k \to 0$ our predictions for the dynamic structure factor for aluminum recover the known hydrodynamical form. We then make predictions for $S_{\alpha\beta}(k,\omega)$ and the adiabatic sound speed of warm dense plastic (CH), which is commonly used as an ablator material in inertial confinement fusion capsules [19]. We extract the sound speeds from each component of the dynamic structure factor and show that in the hydrodynamic limit they converge to a common value – as they should. Finally, the quasi-elastic electron-electron dynamic structure factor is calculated from $S_{\alpha\beta}(k,\omega)$. Such a quantity is in principle directly accessible in X-ray scattering experiments [13].

II. METHODS

In pseudo-atom molecular dynamics (PAMD) the electronic density of the plasma for a given set of nuclear positions is constructed through a superposition of spherically symmetric pseudo-atom electron densities that are identical for all ions of a given species. The pseudo-atom density contains contributions from bound electrons (together with the nucleus, they form the ion) and the electrons that screen the ion [16]. The pseudo-atom electron densities are found using DFT [17, 18, 20], for which we use the Dirac exchange functional [21]. By applying the integral equations of fluid theory to the plasma [17, 20], one can determine the ion-ion pair interaction potentials. These pair potentials are uniquely determined by the pseudo-atom electron densities; there are no adjustable parameters or assumed functional form. The nuclear positions are found with classical molecular dynamics using these pair potentials. The only inputs to PAMD are the plasma density, temperature and composition (i.e. atomic masses, nuclear charges and the number fractions of the species). Our classical MD simulations are carried out in the micro-canonical ensemble. The simulations are guided to equilibrium using velocity rescaling to achieve the target temperature; no thermostat is used during the production phase. Due to the short range nature of the pair interaction potentials for the systems considered here there is no need to use the Ewald summation technique. Specific simulation parameters are given for each calculations presented in section III.

The dynamic structure factor is evaluated by first calculating the Fourier transform of the ionic number density

$$n_\alpha(\boldsymbol{k},t) = \sum_{i=1}^{N_\alpha} \exp(\imath \boldsymbol{k}\cdot\boldsymbol{r}_i(t)) \qquad (1)$$

where there are N_α ions of species α in the simulation with positions $\boldsymbol{r}_i(t)$ at time t. The intermediate scattering function is then constructed

$$F_{\alpha\beta}(k,t) = \frac{1}{\sqrt{N_\alpha N_\beta}} \langle n_\alpha(\boldsymbol{k},t) n_\beta(-\boldsymbol{k},t)\rangle \qquad (2)$$

where the angular brackets imply an average of directions as well as the ensemble average. Finally, the dynamic structure factors are the time Fourier transforms of $F_{\alpha\beta}(k,t)$

$$S_{\alpha\beta}(k,\omega) = \frac{1}{2\pi}\int_{-\infty}^{\infty} dt \exp(\imath\omega t) F_{\alpha\beta}(k,t) \qquad (3)$$

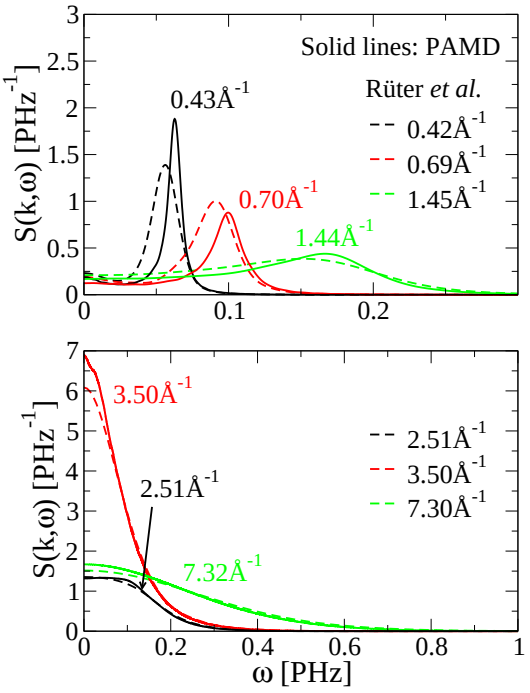

FIG. 1: (color online) $S(k,\omega)$ for aluminum at 5.2 g/cm^3 and 3.5 eV. Solid lines are PAMD calculations and the numbers beside each curve indicate the k-value. The dashed lines are from QMD simulations [10] and the legend indicates their k-values. Despite the very different simulation methods involved, the agreement is good. The differences result from a combination of physical approximations and computational limitations (see text).

III. RESULTS

A. Aluminum plasmas

In figure 1 we compare PAMD calculations of $S_{\alpha\beta}(k,\omega)$ to QMD[1] results [10] for an aluminum plasma at 3.5 eV

[1] QMD – Quantum Molecular Dynamics, refers to Kohn-Sham DFT-MD simulations.

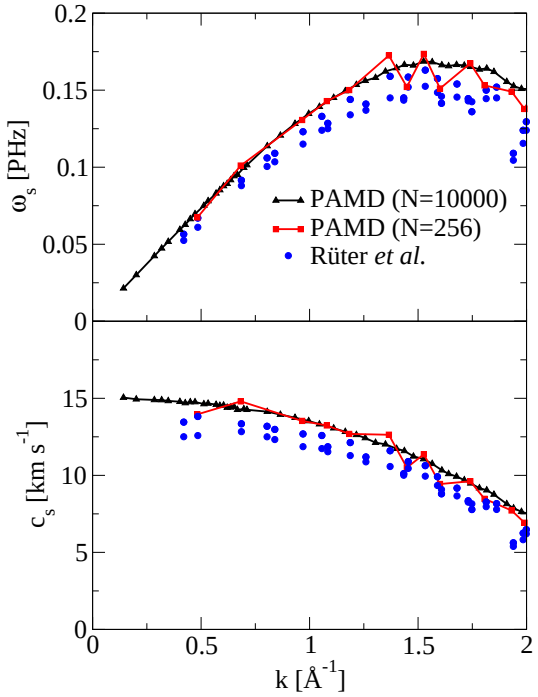

FIG. 2: (color online) Dispersion relation ω_s (top panel) and adiabatic sound speed $c_s = \omega_s/k$ (bottom panel) for aluminum at 5.2 g/cm^3 and 3.5 eV. Solid lines with triangles are PAMD calculations using 10,000 particles. The blue dots are QMD results from [10], where 256 particles were used. For comparison, we also plot the results of a PAMD simulation using 256 particles (solid lines with squares).

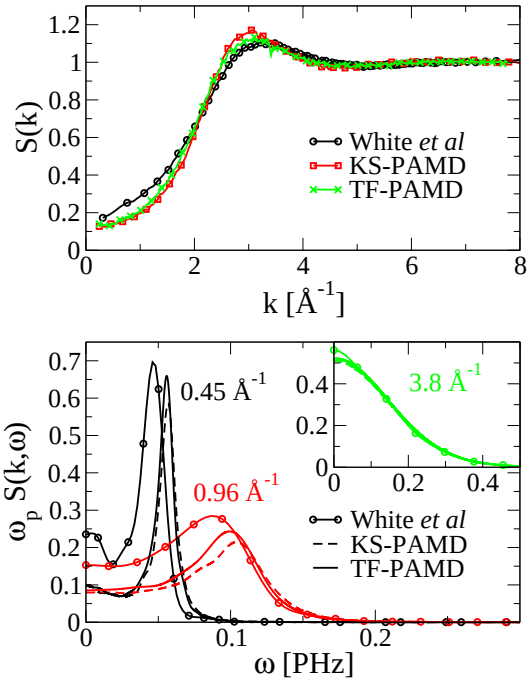

FIG. 3: (color online) Static structure factor (top panel) and $S(k,\omega)$ (bottom panel) for aluminum at 2.7 g/cm^3 and 5 eV compared to TF-DFT-MD simulations [9]. We show PAMD results using both Thomas-Fermi (TF) and Kohn-Sham (KS) functionals. ω_p is the ion plasma frequency. For KS-PAMD $\hbar\omega_p = 0.123$ eV, for TF-PAMD $\hbar\omega_p = 0.125$ eV.

and 5.2 g/cm^3. For the smallest k-vectors[2] both calculations predict a strong ion acoustic (Brillouin) peak, and a small central diffusive (Rayleigh) peak. This is also where the quantitative agreement of the two approaches is at its worst. Increasing k to values corresponding to the first peak in the static structure factor (see figure 5), and beyond, the agreement improves and both methods recover the free particle limit (a Gaussian) at the largest k value.

In figure 2 we show the dispersion relation $\omega_s(k)$ of the ion acoustic peak for the same aluminum plasma compared to the QMD results of [10], and the corresponding sound speed $c_s = \omega_s/k$. The scatter in the QMD data is partly a result of suppression of long time oscillations in $F(k,t)$ using a Gaussian window function [10] with two different choices of the decay time scale. These long time oscillations must also be damped in the PAMD simulations; we apply the method described in [22]. The combination of this method as well as long and large PAMD simulations result in very little numerical noise in ω_s and c_s. The PAMD simulations predict a slightly larger sound speed (15.0 km s^{-1}) than the QMD simulations (12.5–14 km s^{-1}), but the overall agreement is good.

The differences in the predicted $S(k,\omega)$ from the two methods (PAMD and QMD) are likely to be caused by a combination of numerical limitations and physical approximations. The well-converged PAMD simulations used 10,000 particles for a total simulation time of 0.36 ns [3]. In contrast, the QMD simulations of [10] used 256 particles for a total simulation time of 3.08 ps. Due to the expensive nature of the QMD simulations convergence tests using a larger number of particles and longer simulations are impractical. We verified that PAMD simulations using 256 particles and 3.08 ps do not significantly change the resulting sound speed, although it becomes much noisier (figure 2). However, QMD and PAMD should have different size effects due to the different methods involved. A modest reduction of $\sim 2.5\%$ in the PAMD c_s was found when the Dirac exchange potential was replaced by a finite temperature exchange and correlation potential in the local density approximation [23]. One the

[2] The use of periodic boundary conditions in both QMD and PAMD restricts the k values that are accessible to each simulation, hence the slight differences in the k values in figure 1.

[3] We used a cubic simulation cell with a time step of 0.95 fs.

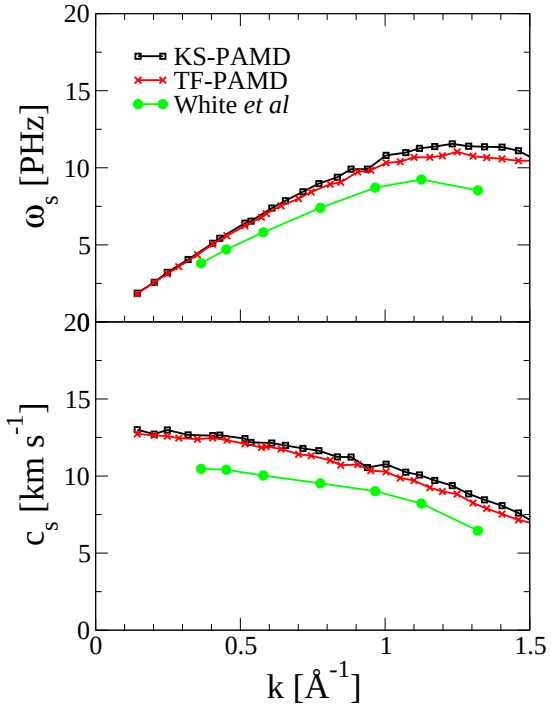

FIG. 4: (color online) Dispersion relation ω_s (top panel) and adiabatic sound speed $c_s = \omega_s/k$ (bottom panel) for aluminum at 2.7 g/cm^3 and 5 eV. We show PAMD results using both Thomas-Fermi (TF) and Kohn-Sham (KS) functionals.

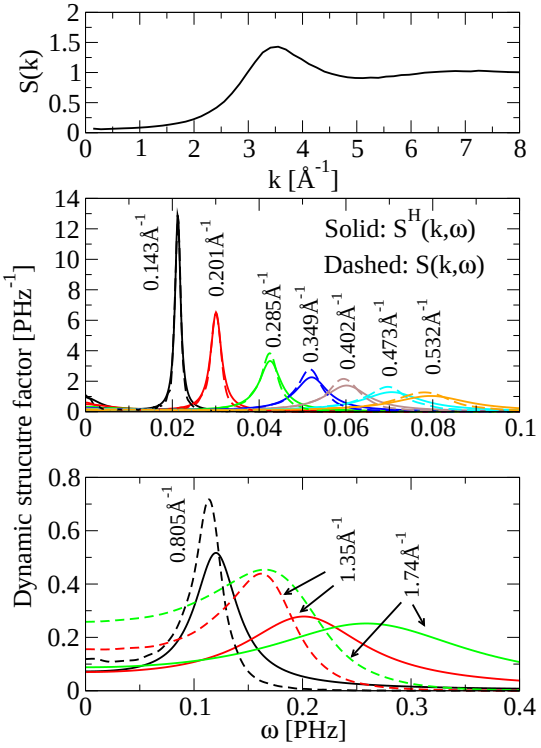

FIG. 5: (color online) Static structure factor (top panel) for aluminum at 5.2 g/cm^3 and 3.5 eV. The bottom two panels show the calculated dynamical structure factor and the hydrodynamical fit (equation (4)). The four fit parameters are determined by a least squares fit of the calculated data for $k = 0.143$ Å^{-1}. On increasing k (values are marked beside the corresponding lines) this hydrodynamical fit begins to deviate from the calculated curves, as is expected.

other hand the QMD simulations [10] used a generalized gradient approximation [24]. Other physical approximations that may affect the results include the superposition approximation in PAMD, and the use of a pseudopotential in the QMD simulations [10]. We note that PAMD does not use a pseudopotential; bound states are treated in the same way as the continuum states. In summary the agreement between the methods is good, given the very different approaches used.

In figure 3 we show the static structure factor and $S(k,\omega)$ for an aluminum plasma at 2.7 g/cm^3 and 5 eV. Both Thomas-Fermi (TF) and Kohn-Sham (KS) PAMD results are shown and compared the DFT-MD simulations of White et al. [9]. The simulations of White et al. used the Thomas-Fermi functional and a pseudopotential derived by inverting the Kohn-Sham equations for bulk aluminum [25]. This effectively corrects the poor behavior of TF-DFT-MD at low temperatures by recovering the proper limit, and makes the TF-DFT-MD behave like KS-DFT-MD at low temperature. The KS and TF-PAMD results are similar, and there is reasonable agreement with the TF-DFT-MD results of White et al. However, the agreement is worse than for the KS-DFT aluminum plasma shown in figure 1. In particular, PAMD gives a smaller value for $S(k,\omega=0)$ than the results of White et al and higher frequencies for the acoustic peak at small k values. The corresponding sound speeds and dispersion relations for are shown in figure 4. TF-PAMD predicts an adiabatic sound speed of 12.7 km/s compared to 10.4 km/s from TF-DFT-MD. Our PAMD simulations used 5000 particles in a cubic simulation cell with a time step of 0.84 fs for a total simulation time of 1.34 ns. In contrast the TF-DFT-MD result used 864 particles with a time step of 0.25 fs for a simulation time of 1.5 ps. The most likely source of the differences observed in figure 3 is either the superposition approximation in PAMD or the pseudopotential in TF-DFT-MD.

In summary, the comparison of PAMD to KS- and OF-DFT-MD simulations of $S_{\alpha\beta}(k,\omega)$ and the corresponding sound speed reveals good to reasonable agreement. The differences are most likely due to physical approximations: the superposition approximation in PAMD, the pseudopotentials in KS- and OF-DFT MD, and the difference choices of exchange and correlations potentials. Numerical limitations of the much more expensive DFT-MD methods may play a part. The dynamic structure factor $S_{\alpha\beta}(k,\omega)$ is a very sensitive test of the forces on the ions. That a parameter-free pair potential method (i.e. PAMD) attains the level of agreement seen with the DFT-MD methods is quite remarkable, and supports the underlying assumptions of PAMD. These compar-

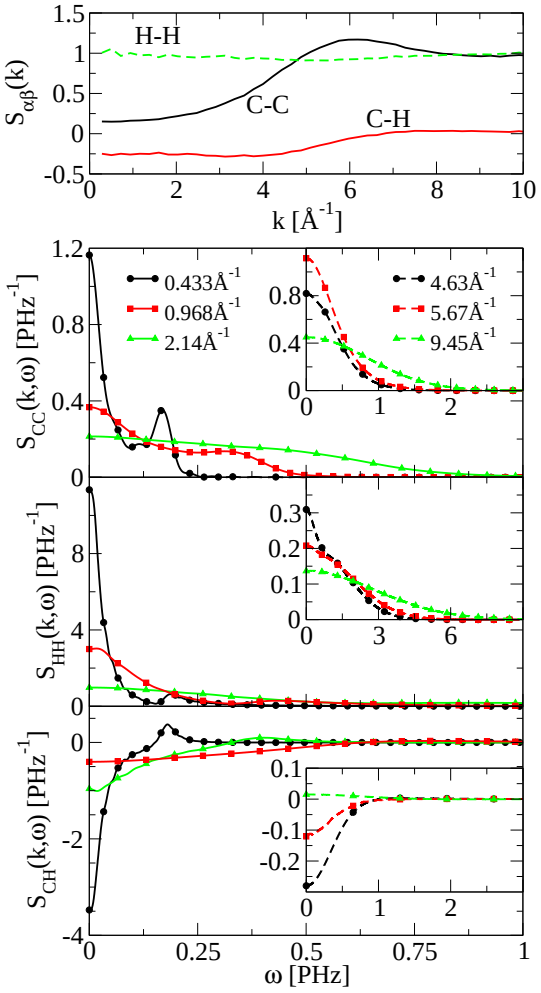

FIG. 6: (color online) Static structure factor from PAMD (top panel) for a carbon-hydrogen mixture at 10 g/cm^3 and 10 eV. The bottom three panels show the dynamic structure factors for C-C, H-H and C-H at various fixed values of k.

isons also give us confidence that predictions of $S_{\alpha\beta}(k,\omega)$ with PAMD are reasonably accurate and that PAMD can be used as a relatively inexpensive tool for investigating $S_{\alpha\beta}(k,\omega)$ in warm dense matter.

In figure 5 we show $S(k,\omega)$ for an aluminum plasma at 3.5 eV and 5.2 g/cm^3 at small k values. For the smallest k value available from the simulation ($k = 0.143$Å^{-1}) we use a least squares fit to the hydrodynamical form of the dynamic structure factor [26]:

$$S^H(k,\omega) = \frac{S(k)}{2\pi}\left[\left(\frac{\gamma-1}{\gamma}\right)\frac{2D_T k^2}{\omega^2+(D_T k^2)^2} + \frac{1}{\gamma}\left(\frac{\Gamma k^2}{(\omega+c_s\,k)^2+(\Gamma\,k^2)^2}+\frac{\Gamma k^2}{(\omega-c_s\,k)^2+(\Gamma\,k^2)^2}\right)\right] \quad (4)$$

The four parameters of this fit are $\gamma = c_P/c_V$, the ratio of specific heats, D_T, the thermal diffusivity, Γ, the sound attenuation coefficient which is related to the kinematic viscosity [26] and c_s, the adiabatic sound speed.

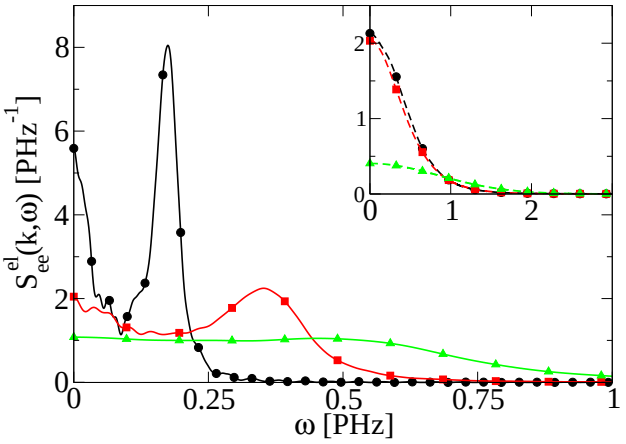

FIG. 7: (color online) Elastic part of the electron-electron dynamic structure factor for CH at 10 eV and 10 g/cm^3. The k-values and line labels in this figure and inset are the same as in figure 6.

In principle, fitting the form (4) to the small-k $S_{\alpha\beta}(k,\omega)$ provides all four material properties. For reference the values of the four fit parameters found for this case are (in atomic units) $\gamma = 1.18$, $D_T = 1.68\times 10^{-2}$, $\Gamma = 3.21\times 10^{-3}$ and $c_s = 6.84\times 10^{-3}$. The agreement between the PAMD $S(k,\omega)$ and the fit is very good. Keeping these parameters fixed, but increasing k we can see that the hydrodynamical fit starts to deviate from the calculated curves, with noticeable differences for $k \gtrsim 0.3$Å^{-1}.

B. Carbon-hydrogen plasma

We now turn to $S_{\alpha\beta}(k,\omega)$ for a carbon-hydrogen mixture relevant to inertial confinement fusion experiments [8]. Figure 6 shows the PAMD $S_{CC}(k,\omega)$, $S_{HH}(k,\omega)$ and $S_{CH}(k,\omega)$ for an equimolar carbon - hydrogen mixture at 10 eV and 10 g/cm^3. Bonds can occur in CH plasmas at lower temperature and density [8]. We have previously shown that the ion-ion pair interaction potentials used in PAMD result in static structure predictions that agree well with QMD calculations under similar conditions for a carbon-hydrogen mixture [20], consistent with the complete breakup of bonds found in [8]. The PAMD simulations here used a total of 8,000 particles and a total simulation time of 0.12ns in a cubic simulation box with time step of 0.068 fs. The partial structure factors $S_{\alpha\beta}(k)$ for the CH plasma (figure 6, top panel) shows that the hydrogen ions are uncorrelated, the carbon ions are moderately coupled, and that there is no sign of incipient bonding in the system. The partial dynamical structure factors $S_{\alpha\beta}(k,\omega)$ reveal significantly different behavior of the carbon and hydrogen ions. The H-H diffusive peak is ∼10 times larger than that of C-C, owing to the much lower mass and charge (i.e. coupling) of the hydrogen. For the same reason the acoustic peak of $S_{HH}(k,\omega)$ is

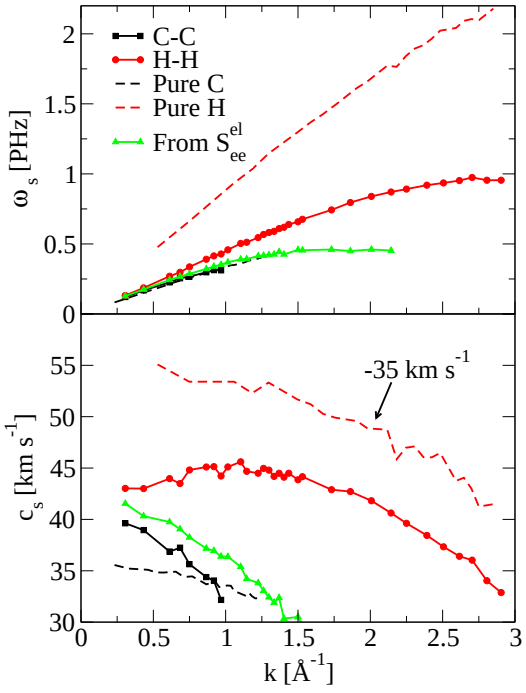

FIG. 8: (color online) Top panel shows the dispersion relations extracted from the PAMD dynamic structure factors $S_{CC}(k,\omega)$, $S_{HH}(k,\omega)$ and $S_{ee}^{el}(k,\omega)$ as well as the dispersion relations for a pure hydrogen and a pure carbon plasma at the same temperature and density as the mixture (10 eV and 10 g/cm^3). In the bottom panel the corresponding adiabatic sound speeds ($c_s = \omega_s/k$) are shown. For clarity, the sound speed for the pure hydrogen case has been shifted by -35 km s^{-1}.

always at a higher frequency than for $S_{CC}(k,\omega)$.

X-ray scattering experiments measure the double-differential cross section which is proportional to the total electron structure factor [27]. For small ω the dominant contribution to this is from quasi-elastic scattering by the bound and screening electrons. This is related to the ion-ion dynamic structure factors by [20, 27–29]

$$S_{ee}^{el}(k,\omega) = \sum_{\alpha,\beta} \sqrt{x_\alpha x_\beta} n_{\alpha,e}^{PA}(k) n_{\beta,e}^{PA}(k) S_{\alpha\beta}(k,\omega) \qquad (5)$$

where the sums are over species index, x_α is the number fraction of species α and $n_{\alpha,e}^{PA}(k)$ is the Fourier transform of the pseudo-atom electron density for species α [20, 28]. The result for the carbon-hydrogen mixture is shown in figure 7. Unlike the pure aluminum cases, the central diffusive (Rayleigh) peak is comparable in magnitude to the acoustic peak at small k. This is due in roughly equal parts to the larger value of $S(k)$ for CH compared to that for Al (see equation (4)), and a larger value of the ratio of specific heats γ.

The dispersion relations and corresponding sound speeds extracted from $S_{CC}(k,\omega)$ and $S_{HH}(k,\omega)$ are shown in figure 8. As $k \to 0$ these sound speeds converge to a common value, as they should in the hydrodynamic limit. Even with these large simulations, at the smallest k value available the two sound speeds still differ by $\sim 8\%$; their average value predicting a sound speed of 41.3 km s^{-1}. For comparison, we also show the dispersion relations and sound speeds for pure hydrogen and pure carbon plasmas at the same density and temperature as the mixture. Also shown in figure 8 is the dispersion relation and sound speed extracted from $S_{ee}^{el}(k,\omega)$. Qualitatively this follows the carbon-carbon result but is shifted to larger sound speeds.

As k increases from the hydrodynamic limit the sound speeds for hydrogen and carbon split into fast (H) and slow (C) sounds, with hydrogen showing a slight positive dispersion (figure 8). This phenomenon, known as "fast sound", was first predicted in molecular dynamics simulations of liquids [30] and later observed in neutron scattering experiments on a cryogenic He-Ne mixture [31] and in a low-density, hot Be-Au plasma [32]. To our knowledge, this is the first time the fast sound phenomenon has been predicted in the warm dense matter regime. This effect arises as a consequence of transitioning from the hydrodynamic to kinetic regimes [33], where the behavior of particles of each species is less collective and reflects more their different masses and interaction potentials.

IV. CONCLUSIONS

In conclusion, we have demonstrated that the recently developed pseudo-atom molecular dynamics simulation method for warm dense matter can be used to investigate the ion-ion dynamic structure factor, giving results that agree well with the much more computationally expensive KS-DFT-MD methods. A comparison with TF-DFT-MD simulations also gave reasonable agreement. These comparisons give us confidence that PAMD can be used as reasonably accurate and relatively inexpensive tool to investigate the properties of $S_{\alpha\beta}(k,\omega)$ in warm dense matter. In the hydrodynamic limit, the known form of the ion-ion dynamic structure factor is recovered by PAMD simulations for an aluminum plasma. We have used PAMD to make predictions of the ion-ion dynamic structure factor and the adiabatic sound speed of a warm dense mixture of carbon and hydrogen. From these we have calculated the quasi-elastic part of the electron-electron dynamic structure factor, a quantity that is measurable in X-ray scattering experiments.

Acknowledgments

We are grateful to H. Rüter for providing the QMD aluminum data [10], to T. Sjostrom for providing the subroutine for calculation of the finite temperature exchange and correlation potential, and to J. Daligault for useful discussions. This work was performed under the auspices of the United States Department of Energy under contract DE-AC52-06NA25396.

[1] N. Nettelmann, A. Becker, B. Holst, and R. Redmer. *The Astrophysical Journal*, 750:52, 2012.

[2] Report of ReNew workshop. *Basic research needs for high energy density laboratory physics*. U.S. Department of Energy, 2009. http://science.energy.gov/~/media/fes/pdf/workshop-reports/hedlp_brn_workshop_report_oct_2010.pdf.

[3] S. Atzeni and J. Meyer-Ter-Vehn. *The physics of inertial fusion*. Clarendon Press-Oxford, 2004.

[4] J. D. Kress, James S. Cohen, D. A. Horner, F. Lambert, and L. A. Collins. Viscosity and mutual diffusion of deuterium-tritium mixtures in the warm-dense-matter regime. *Phys. Rev. E*, 82:036404, Sep 2010.

[5] D. A. Horner, J. D. Kress, and L. A. Collins. Quantum molecular dynamics simulations of warm dense lithium hydride: Examination of mixing rules. *Phys. Rev. B*, 77:064102, Feb 2008.

[6] D. A. Horner, J. D. Kress, and L. A. Collins. Effects of metal impurities on the optical properties of polyethylene in the warm dense-matter regime. *Phys. Rev. B*, 81:214301, Jun 2010.

[7] J.-F. Danel and L. Kazandjian. Equation of state of a dense plasma by orbital-free and quantum molecular dynamics: Examination of two isothermal-isobaric mixing rules. *Phys. Rev. E*, 91:013103, Jan 2015.

[8] Sebastien Hamel, Lorin X. Benedict, Peter M. Celliers, M. A. Barrios, T. R. Boehly, G. W. Collins, Tilo Döppner, J. H. Eggert, D. R. Farley, D. G. Hicks, J. L. Kline, A. Lazicki, S. LePape, A. J. Mackinnon, J. D. Moody, H. F. Robey, Eric Schwegler, and Philip A. Sterne. Equation of state of $ch_{1.36}$: First-principles molecular dynamics simulations and shock-and-release wave speed measurements. *Phys. Rev. B*, 86:094113, Sep 2012.

[9] T. G. White, S. Richardson, B. J. B. Crowley, L. K. Pattison, J. W. O. Harris, and G. Gregori. *Phys. Rev. Lett.*, 111:175002, 2013.

[10] H. R. Rüter and R. Redmer. *Phys. Rev. Lett.*, 112:145007, 2014.

[11] J. Vorberger, Z. Donko, I. M. Tkachenko, and D. O. Gericke. *Phys. Rev. Lett.*, 109:225001, 2012.

[12] James P. Mithen, Jérôme Daligault, and Gianluca Gregori. *Phys. Rev. E*, 83:015401, 2011.

[13] S. H. Glenzer and R. Redmer. *Rev. Mod. Phys.*, 81:1625, 2009.

[14] U. Zastrau, T. Burian, J. Chalupsky, T. Döppner, T.W.J. Dzelzainis, R.R. Fäustlin, C. Fortmann, E. Galtier, S.H. Glenzer, G. Gregori, L. Juha, H.J. Lee, R.W. Lee, C.L.S. Lewis, N. Medvedev, B. Nagler, A.J. Nelson, D. Riley, F.B. Rosmej, S. Toleikis, T. Tschentscher, I. Uschmann, S.M. Vinko, J.S. Wark, T. Whitcher, and E. Förster. Xuv spectroscopic characterization of warm dense aluminum plasmas generated by the free-electron-laser flash. *Laser and Particle Beams*, 30:45–56, 3 2012.

[15] J. Vorberger and D.O. Gericke. Effective ion–ion potentials in warm dense matter. *High Energy Density Physics*, 9(1):178 – 186, 2013.

[16] C. E. Starrett, J. Daligault, and D. Saumon. *Phys. Rev. E*, 91:013104, 2015.

[17] C. E. Starrett and D. Saumon. *Phys. Rev. E*, 87:013104, 2013.

[18] C. E. Starrett and D. Saumon. *High Energy Dens. Phys.*, 10:35, 2014.

[19] B. A. Hammel, S. W. Haan, D. S. Clark, M. J. Edwards, S. H. Langer, M. M. Marinak, and M. V. Patel. *High energy density physics*, 6:171, 2010.

[20] C. E. Starrett, D. Saumon, J. Daligault, and S. Hamel. *Phys. Rev. E*, 90:033110, 2014.

[21] P. A. M. Dirac. *Proc. Camb. Phil. Soc.*, 26:376, 1930.

[22] J.P. Mithen. *PhD thesis, available at http://www.surrey.ac.uk/physics/people/james_mithen/*, 2012.

[23] Valentin V. Karasiev, Travis Sjostrom, James Dufty, and S. B. Trickey. *Phys. Rev. Lett.*, 112:076403, 2014.

[24] John P. Perdew, Kieron Burke, and Matthias Ernzerhof. Generalized gradient approximation made simple. *Phys. Rev. Lett.*, 77:3865–3868, Oct 1996.

[25] Chen Huang and Emily A. Carter. Transferable local pseudopotentials for magnesium, aluminum and silicon. *Phys. Chem. Chem. Phys.*, 10:7109–7120, 2008.

[26] J.-P. Hansen and I.R. McDonald. *Theory of simple liquids, Third edition*. Academic Press, 2006.

[27] J. Chihara. *J. Phys.: Condens. Matter*, 12:231, 2000.

[28] A. N. Souza, D. J. Perkins, C. E. Starrett, D. Saumon, and S. B. Hansen. *Phys. Rev. E*, 89:023108, 2014.

[29] Kathrin Wünsch, Jan Vorberger, G Gregori, and Dirk O Gericke. X-ray scattering as a probe for warm dense mixtures and high-pressure miscibility. *EPL (Europhysics Letters)*, 94(2):25001, 2011.

[30] Jürgen Bosse, Gianni Jacucci, Marco Ronchetti, and Walter Schirmacher. *Phys. Rev. Lett.*, 57:3277–3279, 1986.

[31] W. Montfrooij, P. Westerhuijs, V. O. de Haan, and I. M. de Schepper. *Phys. Rev. Lett.*, 63:544–546, 1989.

[32] S. H. Glenzer, C. A. Back, K. G. Estabrook, R. Wallace, K. Baker, B. J. MacGowan, B. A. Hammel, R. E. Cid, and J. S. De Groot. Observation of two ion-acoustic waves in a two-species laser-produced plasma with thomson scattering. *Phys. Rev. Lett.*, 77:1496–1499, Aug 1996.

[33] Stefano Cazzato, Tullio Scopigno, Taras Bryk, Ihor Mryglod, and Giancarlo Ruocco. Crossover between hydrodynamic and kinetic modes in binary liquid alloys. *Phys. Rev. B*, 77:094204, Mar 2008.